Supplementary Information for:

Active Phase Evolution in Single Ni/Al_2O_3 Methanation Catalyst Bodies Studied in Real Time using Combined μ-XRD-CT and μ-Absorption-CT

Matthew G. O'Brien[†], Simon D. M. Jacques[†], Marco Di Michiel[‡], Paul Barnes[¥], Bert M. Weckhuysen[*†] and Andrew M. Beale[*†]

[†] *Inorganic Chemistry and Catalysis Group, Debye Institute for NanoMaterials Science, Utrecht University, Universiteitsweg 99, 3584 CG, The Netherlands*

[‡] *The European Synchrotron Facility, 6 Rue Jules Horowitz, 38000, Grenoble, France*

[¥] *Department of Chemistry, University College London, 20 Gordon Street, London, WC1H 0AJ, UK*
Department of Crystallography, Birkbeck College, Malet Street, London WC1E 7HX, UK

[*] Author to whom correspondence should be addressed:

Email: a.m.beale@uu.nl; b.m.weckhuysen@uu.nl

Fax: 00 31 (0) 30-251-2027

S1. Analysis of temperature profile over the catalyst body

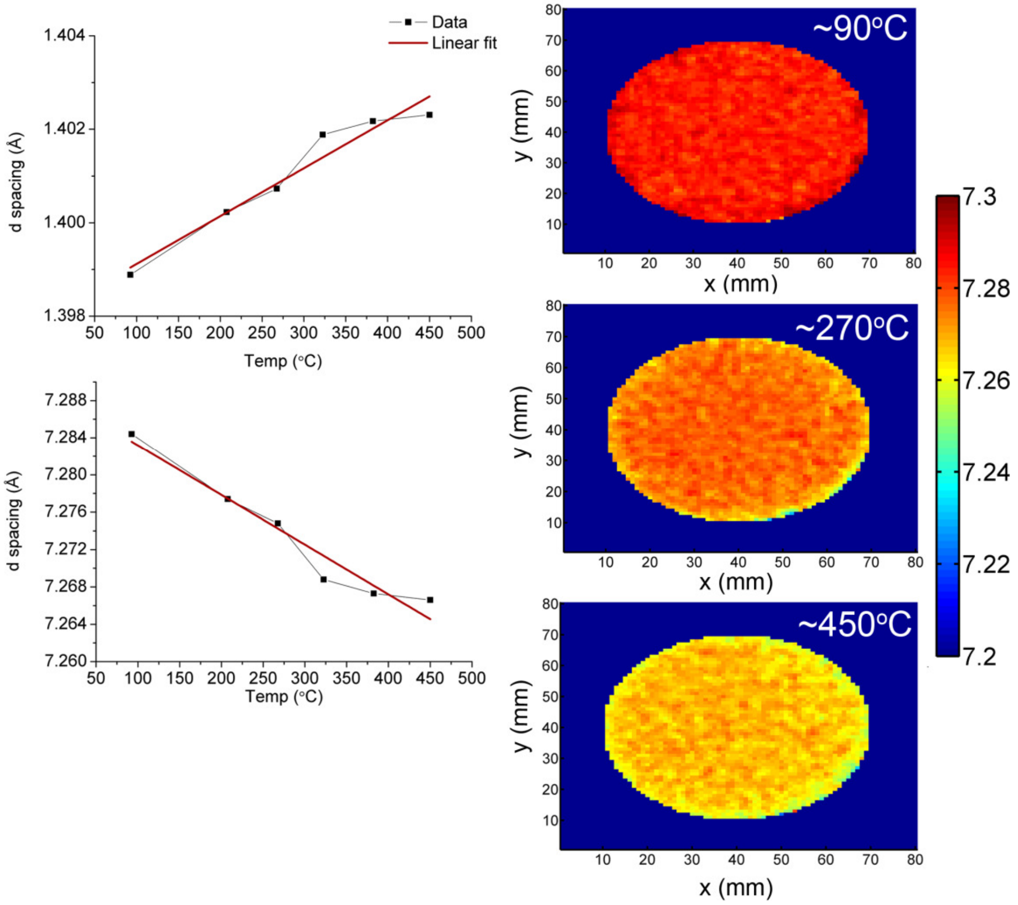

Figure S1: 1 dimensional plots of the variation in the d-spacing/2θ position of the strong (2 0 0) reflection of γ-Al_2O_3 (left) and 2D plots of the variation in 2θ ° over the catalyst body at selected temperature in this range (right). Note that a common scale is used for comparison of the 2D plots.

Initially in Figure S1 the variation of the strongest (2 0 0) peak position is demonstrated as a function of temperature. The variation in 2θ ° over the entire catalyst body is then given at several temperatures. It can be seen from these plots that whilst there is a very slight increase in temperature towards the outside of the catalyst bed (which is to be expected from any externally heating furnace) the heat guns provide even heating over the entire catalyst bed and do not create any artificial gradients or heat spots.

S2. Pattern matching of the minority phases located in the catalyst body prior to oxidation

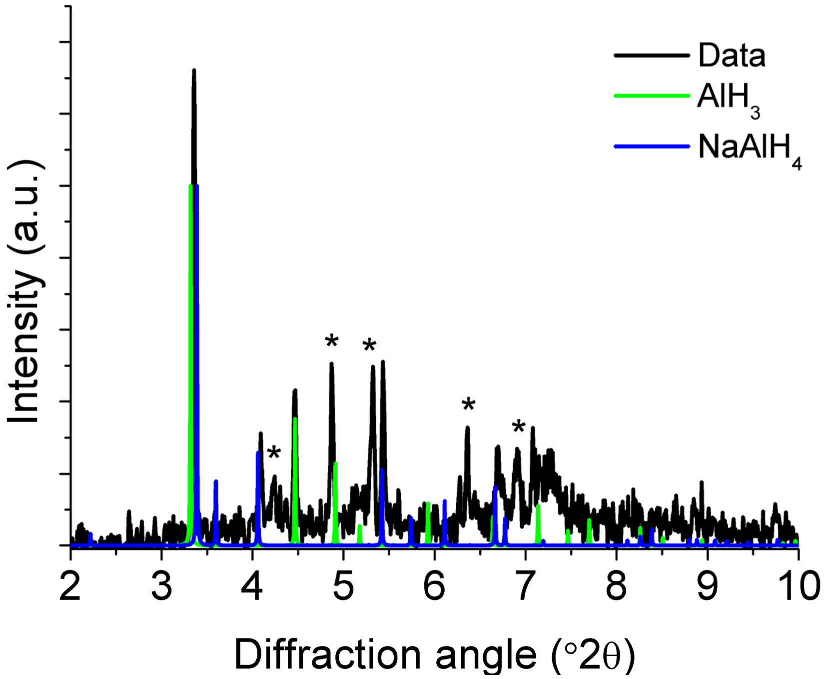

Figure S3: (a) Individual diffraction pattern of the series of phases located in the small portion of the catalyst body marked (●) in Figure 1 prior to oxidation along with simulated patterns of the phases which best fit the data. Unassigned peaks are marked *.

S3. Summed diffraction patterns during the reduction the catalyst in N_2

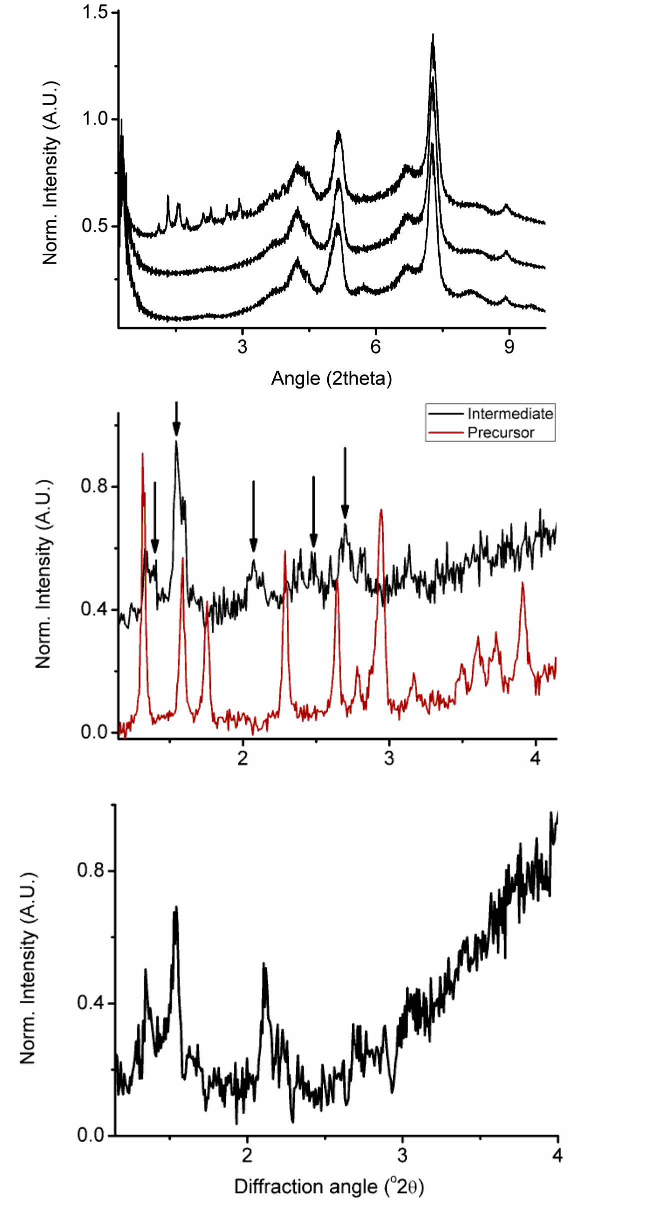

Figure S3: TOP: Summed 1D XRD images of the entire catalyst slice taken during the treatment in N_2, the consumption of the precursor and production of metallic Ni can be observed. **Middle:** Comparative single 1D XRD images from two parts of the catalyst during the first N_2 scan, the formation of an intermediate phase in one part of the catalyst slice is indicated by the arrows. **Bottom:** Summed diffraction images from the weakly scattering central portion of the catalyst demonstrating the formation of the intermediate species.

S4: Discussion regarding CT reconstruction and time resolution within the sample

For data in which the intensity of the signal changes during the recording of the sinogram, artifacts can be observed within the computed tomography reconstruction of the image. Examples of these for the case in which the majority of the material is concentrated at the outside of the sample (as is the case for the measurements presented in the paper) are given in Figure S4.

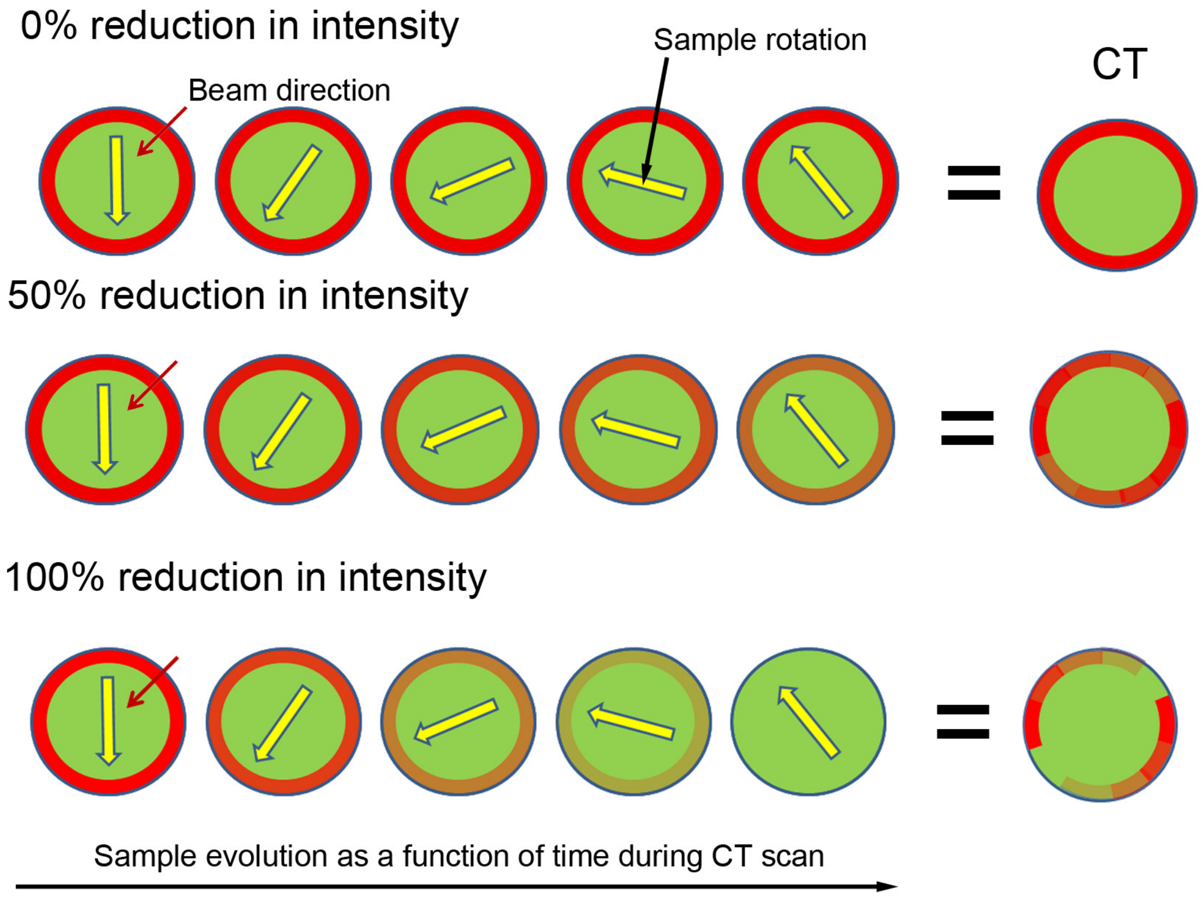

Figure S5: Demonstration of the effect of reduction in signal intensity due to phase consumption during a CT scan. In each case the time frame is the same but the reduction in intensity is different. The resulting CT image is also given.

S5 The formation of NiO in the centre of the catalyst body

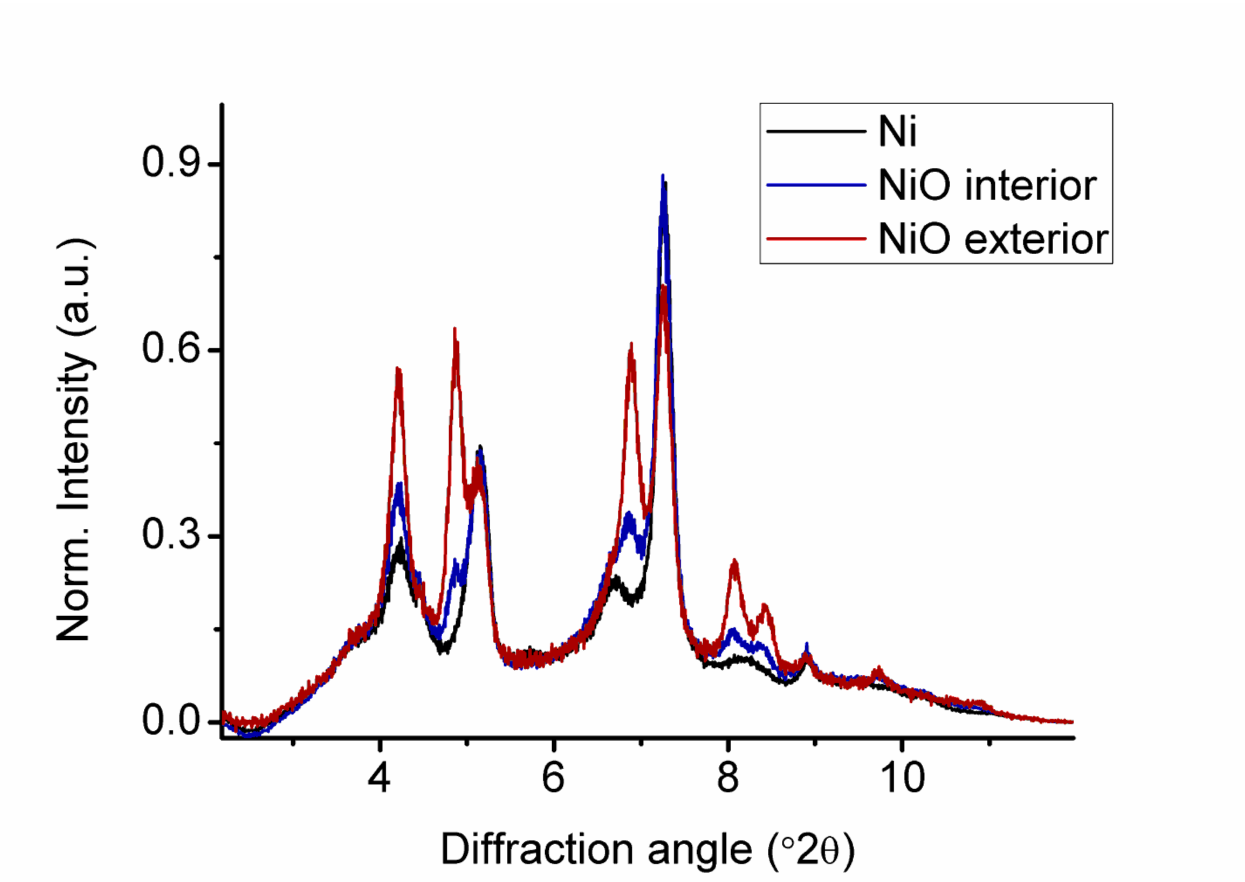

Figure S5: The summed XRD plot of the interior of the pellet clearly demonstrates the presence of NiO after oxidation. For comparison the summed plot from the exterior of the pellet and from a sample containing metallic Ni are also given.

S6. Comparative pattern matching of several crystal structures of γ-Al_2O_3

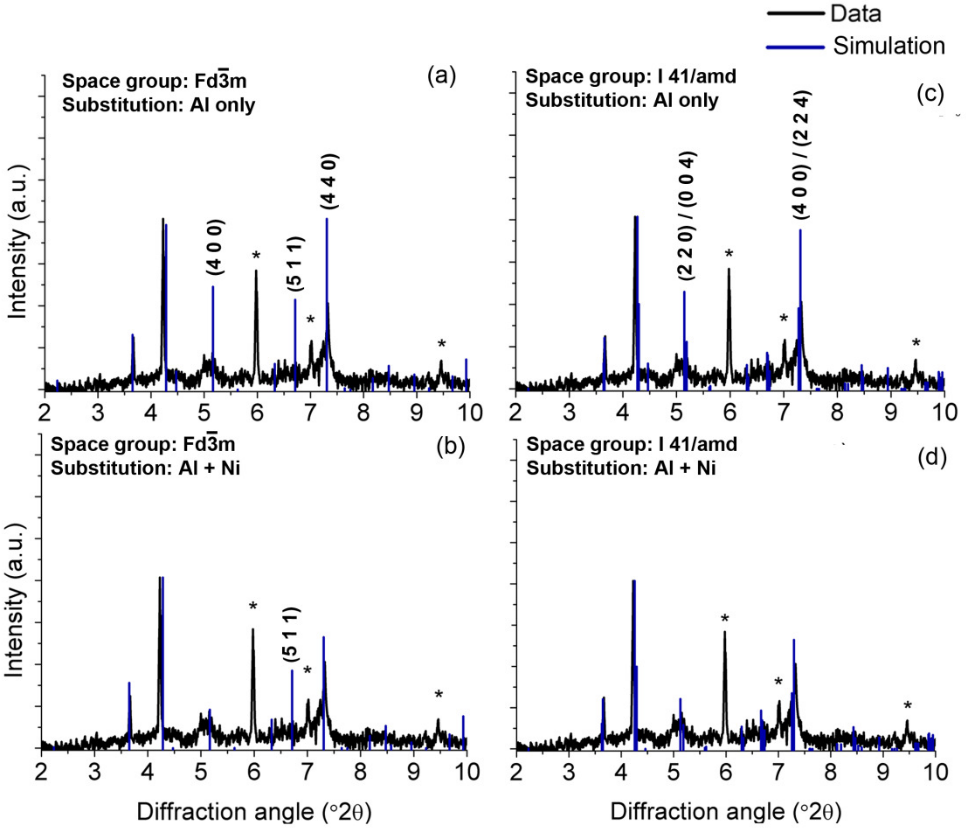

Figure S6: individual 1D XRD patterns for the region of the extrudate containing minority phases after treatment in O_2 along with several simulated patterns. The reflections with the most significant mismatch in intensity are labeled. The phase marked * remains unidentified.

Figure S3 demonstrates several simulations for γ-Al_2O_3 compared with a single XRD patterns from the portion of the catalyst containing the minority phases. (a) simulates the 'usual' cubic γ-Al_2O_3 and results in several intensity mismatches compared to the data. (b) Substitution of 24% of octahedral and 40% of tetrahedral aluminum sites for Ni corrects several of these issues but the peak at (5 1 1) remains too intense in the simulation. (c) changing to the tetragonally distorted form of γ-Al_2O_3 (structure obtained from the inorganic crystal structure database – code 68771)[1,2] then solves this problem and finally (d) repeats the same substitution of Ni as in (b) to obtain a close match to the XRD data. Thus this oxidized minority phase appears to be related to spinel solid solutions (such as $NiAl_2O_3$) which are formed *via* co-precipitation and sol-gel techniques[3] and indicates that there may be a different chemical process occurring in this part of the catalyst where 'normal' γ-Al_2O_3 was not formed during the initial production of the catalyst.

S7. comparison of 1D XRD patterns after N_2 and H_2 treatment

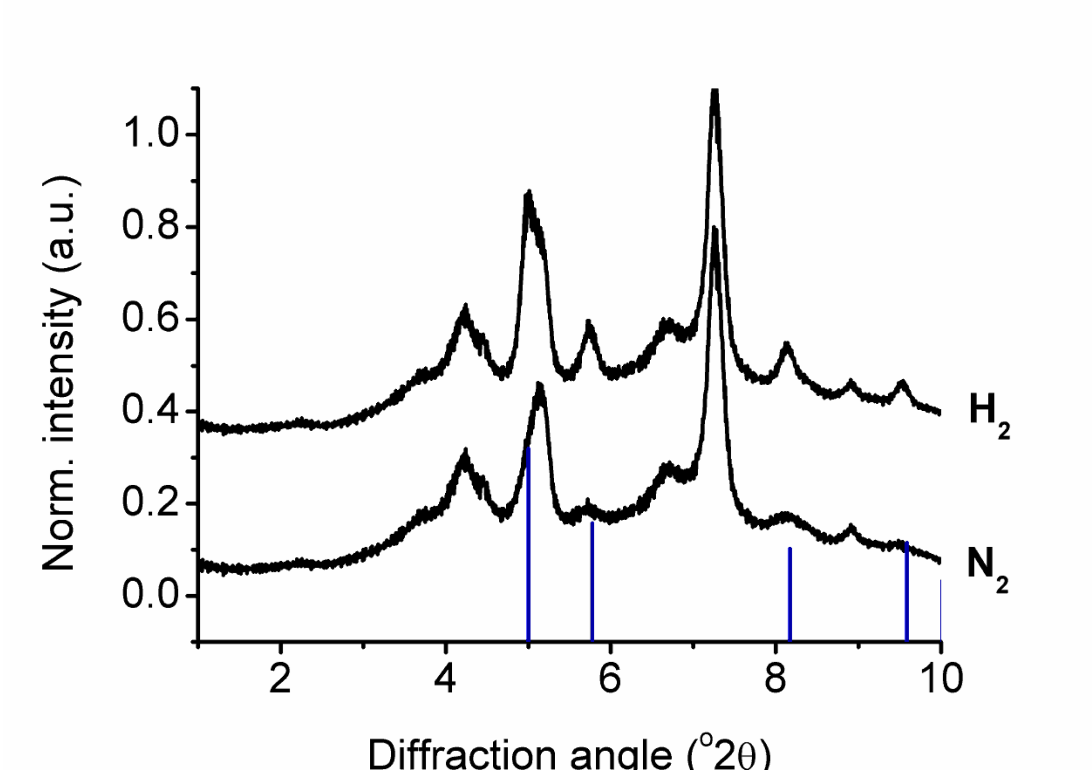

Figure S7: A comparison of the summed 1D XRD pattern for the entire catalyst slice after treatment in N_2 and H_2. There is clearly far more scattering from metallic Ni after treatment in H_2 (the simulated pattern of cubic fcc Ni is given in blue).

References

[1] Li, D. Y.; O’Connor, B. H.; Roach, G. I. D.; Cornell, J. B. XVth Congress of the International Union of Crystallography (Bordeaux); 1990, (Abstracts Vol. C-61)

[2] Paglia, G.; Buckley, C. E.; Rohl, A. L.; Hunter, B. A.; Hart, R. D.; Hanna, J. V.; Byrne, L. T. Phys. Rev. B 2003, 68.

[3] Li, G. H.; Hu, L. J.; Hill, J. M. Appl. Catal. A-Gen. 2006, 301, 16.